JTTEE5 11:375–379

Thermal Properties and Microstructure of a Plasma Sprayed Wollastonite Coating

Xuanyong Liu and Chuanxian Ding

(Submitted 16 January 2001; in revised form 14 April 2001)

Wollastonite coatings were deposited using an atmospheric plasma spraying technique. The microstructure and phase compositions of the coating before and after heat treatment were investigated using scanning electron microscopy (SEM), x-ray diffraction (XRD), and differential thermal analysis (DTA) technologies, respectively. In addition, the coefficient of thermal expansion and thermal diffusivity of the coating were also investigated. Crystalline wollastonite, glassy phase, and tridymite (SiO_2) were observed in the coating. Tridymite (SiO_2) likely reacted with other composites such as CaO and glassy phase to form crystalline wollastonite when the coating was heated at about 882 °C. During the first thermal cycle, the coefficient of thermal expansion of the coating decreased dramatically between 700 and 850 °C and the thermal diffusivity of the coating was $2.7\text{-}3.1 \times 10^{-3}\,cm^2/s$ between 20 and 1000 °C. During the second thermal cycle, the coefficient of thermal expansion of the coating increased slightly between room temperature and 1000 °C and the thermal diffusivity of the coating increased by about 20% compared with that of the first thermal cycle. The atmospheric plasma sprayed Wollastonite coating may be used as thermal barrier coating.

Keywords heat treatment, thermal diffusivity, thermal expansion, Wollastonite coating

1. Introduction

Wollastonite ($CaSiO_3$), a common mineral of metamorphosed limestones and similar assemblages,[1] is an important substance in ceramic and cement industries.[2] Many favorable properties such as low shrinkage, good strength, lack of volatile constituents, body permeability, fluxing characteristics, whiteness, and acicular shape make wollastonite useful in several ceramic and other applications.[3,4] Wollastonite ($CaSiO_3$) ceramic is also a candidate material for high frequency insulators.[5] One of the other possible applications of wollastonite ($CaSiO_3$) ceramic is as a medical material for artificial bone and dental root because of its good bioactivity and biocompatibility.[6-9]

To obtain a medical material for artificial bone, wollastonite coating was prepared on Ti-6Al-4V substrate by atmospheric plasma spraying. The authors found that the atmospheric plasma sprayed wollastonite was of excellent bioactivity and biocompatibility. In this research, the atmospheric plasma sprayed wollastonite coating showed thermophysical properties that were different from bulk materials. Indeed, the thermophysical properties of plasma sprayed coatings are very important in their application. Thermal expansion mismatch between the base material and coating contributes to the development of the residual stresses during the manufacturing process.[10,11] Thermal diffusivity of the coating is a key parameter to applications as thermal barriers.[12-14] Low thermal diffusivity is necessary for use as a thermal barrier coating. Therefore, interest exists in investigating thermal expansion and thermal diffusivity of the atmospheric plasma sprayed wollastonite coating.

The objective of this work was to investigate thermophysical properties such as thermal expansion and thermal diffusivity, examine the microstructure of the plasma sprayed wollastonite coating, and discuss the relationship between the coating properties and microstructure.

2. Experimental Details

2.1 Plasma Spraying

Commercially available wollastonite powder (Ming Hua Minerals Co., Ltd., Liyang Jiangsu Province, China), with typical size ranges of 10-100 μm was used. An atmospheric plasma spray (APS) system with a Sulzer F4 gun (A-2000, Sulzer Metco AG, Switzerland) was used to produce wollastonite coating onto Ti-6Al-4V substrate of dimensions 10 × 10 × 2 mm for metallographic observation and cylindrical (ϕ25.4 mm) substrate for bond strength measurements. The modified spray parameters are listed in Table 1. Before plasma spraying, the substrates were first ultrasonically cleaned in acetone, and then grit blasted using corundum sand of F60 grade (particle mean size about 250 μm).

Coatings to 6 mm thickness were also prepared on aluminum substrate of dimensions 100 × 50 × 2 mm for measurement of thermophysical properties. The aluminum substrate was first ultrasonically cleaned in acetone, and then roughened by a light grit blast using corundum sand. The back of substrate was cooled using water during plasma spraying. The spray parameters are same as those listed in Table 1. After plasma spraying, the 6 mm thick coating was carefully removed from the substrate. It is easy to remove the thick coating from the roughened aluminum substrate using a thin razor because of the poor bonding between the thick coating and the substrate.

Xuanyong Liu and **Chuanxian Ding**, Plasma Spray Laboratory, Shanghai Institute of Ceramics, Chinese Academy of Sciences, Shanghai 200050, China. Contact e-mail: lxyong@citiz.net.

2.2 Phase Identification and Microstructure Analysis

Two samples were heat treated at 700 and 900 °C, respectively, in air for 1 h, then cooled to room temperature in a furnace. The samples for metallographic observation were first cut perpendicular to the coating surface with a low-speed saw, and polished using a grind/polish system (model YM11-15/6, Lanzhou, China) down to a final finish of 0.6 μm with a diamond abrasive paste. After metallographic polishing, the cross-sectioned samples were observed under a scanning electron microscope with electron probe x-ray microanalysis (EPMA), (model 8705QH$_2$, Shimadzu, Japan). The phase compositions of the as-sprayed and heat-treated coating were measured using an x-ray diffractometer (D/Max-rB, Rigaku, Japan).

2.3 Bond Strength Test

The tensile adhesion test (TAT) specified by ASTM C 633-79[15] was used to measure the tensile bonding strength of the coating. In performing this test, two identical cylindrical Ti-6Al-4V rods (diameter of 25.4 mm and length of 25.4 mm) were prepared, one with coating (about 400 μm thick) on a flat surface and the other without coating. The flat surface of the uncoated rod, which was to be bonded to the coated rod, was sandblast-roughened to enhance resin adherence. A thin layer of E-7 adhesive glue (Shanghai, China), which has a tensile fracture strength of more than 70 MPa, was applied. After the two rods were carefully aligned, a compressive stress was applied to both rods to ensure an intimate contact between resin and the two surfaces. After 4 h of curing at 120 °C in an oven at ambient atmosphere, the bonded rods were bench cooled to room temperature. The tensile bonding strength was measured using a materials tester (50 kN load cell; model 11/2612, Germany) at a crosshead speed of 1 mm/min. The value obtained represented an average of five test data.

Table 1 Spray Parameters

Plasma gas Ar	40 slpm	Powder feed rate	25 rpm
Plasma gas H$_2$	12 slpm	Current	500 A
Spray distance	90 mm	Voltage	75 V
Powder carrier gas Ar	3.0 slpm		

2.4 Thermophysical Properties Tests

The differential thermal analysis (DTA) measurements of the wollastonite powder and the coating without the substrate were carried out in air with 5 °C/min heating rate between room temperature and 1000 °C using a thermal analyzer (model STA-429, Netzsch, Germany). Three samples were cut and polished to dimensions 4 × 4 × 50 mm for thermal expansion measurements. Thermal expansion measurements were carried out in air using an alumina pushrod dilatometer (model 402E S/3, Netzsch). Heating rates of 5 °C/min were used and the heating/cooling cycles ranged between 20 and 1000 °C. Three samples were also machined to disk shape (10 mm in diameter and 1.2 mm thick) for thermal diffusivity measurements. The thermal diffusivity was measured using the laser-flash method (model TC-3000, ULVAC, Yokohama, Japan) in vacuum (10^{-5} torr).

3. Results

Figure 1 shows scanning electron microscopy (SEM) micrographs of the polished cross sections of the as-sprayed and heat-treated wollastonite coating on Ti-6Al-4V substrate. The cross-sectional view of the coating revealed slight lamellar structure with a few pores and microcracks. No obvious coating/substrate interfacial separation was observed, which indicated good bonding between the coating and the substrate. The bond strength of the as-sprayed wollastonite coating measured according to ASTM C-633 was about 39 MPa (the thickness of the coating is

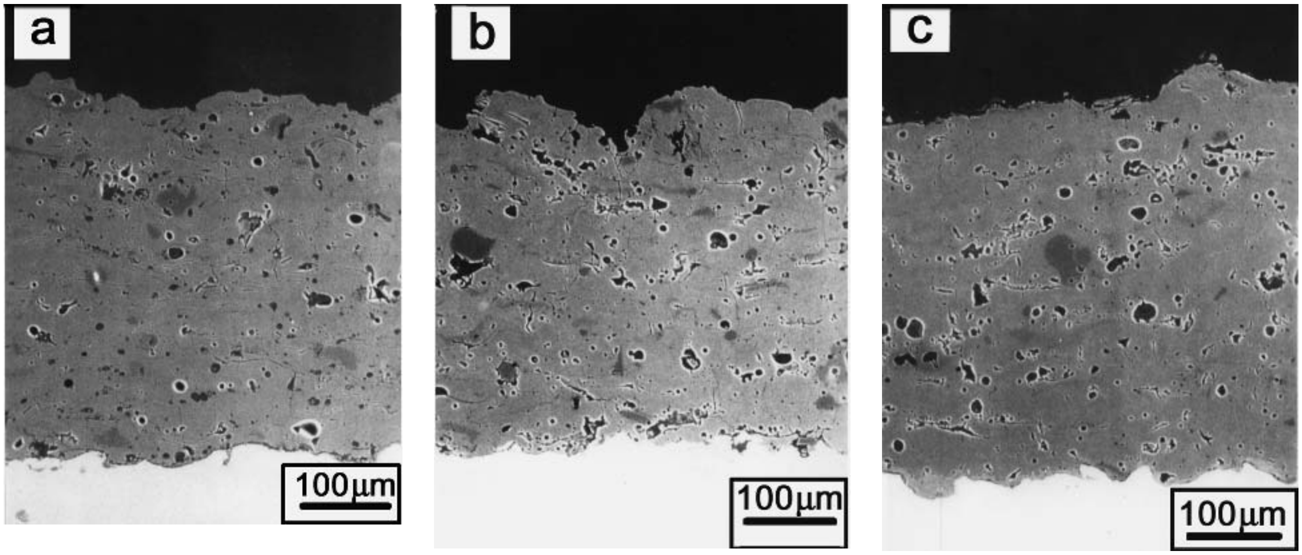

Fig. 1 SEM micrographs of polished cross sections of the wollastonite coating on Ti-6Al-4V substrate: **(a)** as-sprayed, **(b)** heat treated at 700 °C for 1 h, and **(c)** heat treated at 900 °C for 1 h

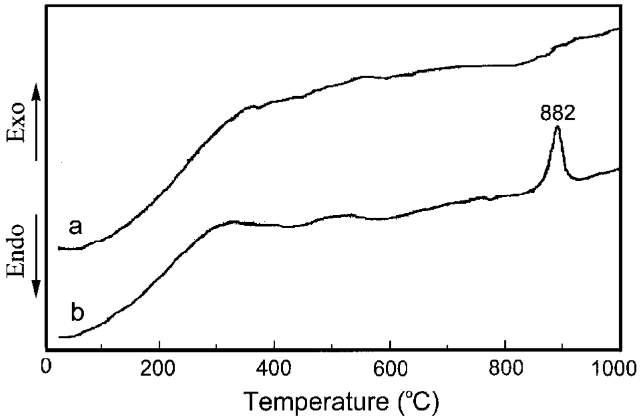

Fig. 2 DTA curves of (a) wollastonite powder and (b) wollastonite coating

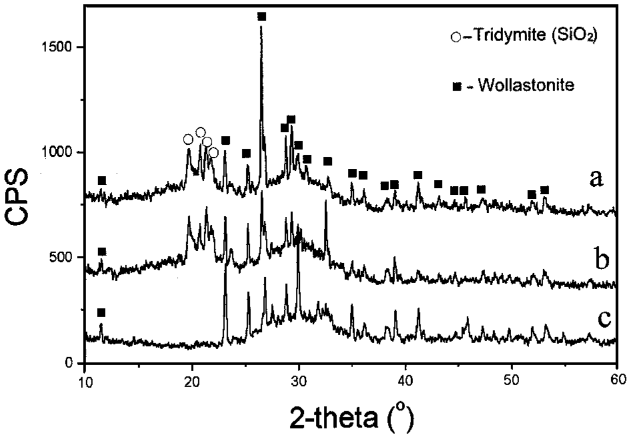

Fig. 3 XRD patterns of the wollastonite coating: **(a)** as-sprayed; **(b)** heat treated at 700 °C for 1 h, and **(c)** heat treated at 900 °C for 1 h

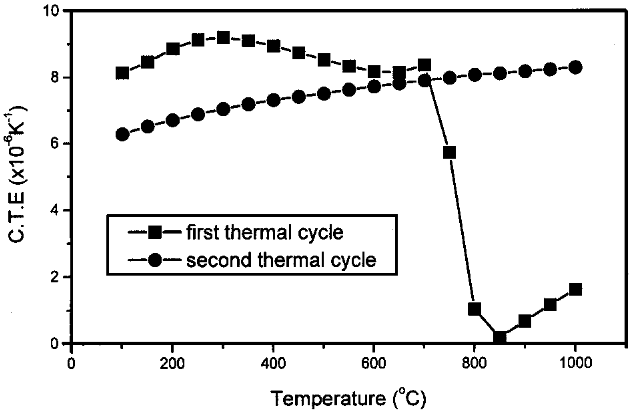

Fig. 4 CTE curves of the wollastonite coating during the first and second thermal cycles

about 400 μm). From Fig. 1, it can be seen that no obvious change in the microstructure of the coating was observed after heat treatment. It is especially noteworthy that the bonding between the coating and Ti-6Al-4V substrate is still very good after the heat treatment. The bond strength of the wollastonite coating, which was heat treated at 900 °C for 1 h, was about 33 MPa (the thickness of the coating has still retained at about 400 μm).

The differential thermal analysis (DTA) curves of the wollastonite powder and the coating are presented in Fig. 2. The DTA curves show that the wollastonite powder had no chemical reactivity from room temperature to 1000 °C (Fig. 2a), whereas an obvious exothermic reaction occurred in the wollastonite coatings at about 882 °C (Fig. 2b). This feature will be discussed below.

The x-ray diffraction (XRD) patterns of the wollastonite coating in the as-sprayed condition and after heat treatment are shown in Fig. 3. Figure 3 shows some sharp peaks and an obvious glass bulge, which is indicative of the existence of glassy phase and crystalline wollastonite in the coating before and after heat treatment. Tridymite (SiO_2) patterns appeared also in the as-sprayed and heat-treated coating at 700 °C (Fig. 3a,b) and disappeared completely after the heat treatment for 1 h at 900 °C (Fig. 3c). In addition, our previous work proved the existence of CaO in the coating by transmission electron microscope (TEM). It should also be noted that the relative height of the peaks, which represent various crystalline planes of wollastonite, changes with the increases in the temperature of heat treatment, which may be indicative of the decrease in the preference of crystalline orientation.

The coefficient of thermal expansion (CTE) of the wollastonite coating in the longitudinal direction (parallel to the substrate surface) during the first and second thermal cycle is shown in Fig. 4. During the first thermal cycle, the CTE of the coating is almost constant up to 700 °C and then decreases dramatically between 700 °C and approximately 850 °C, after which it increases gradually again. However, during the second thermal cycle, the CTE of the wollastonite coating increases slightly between room temperature and 1000 °C.

The thermal diffusivity of the wollastonite coating in the latitudinal direction (perpendicular to the substrate surface) during the first and second thermal cycle is presented in Fig. 5, which shows that the thermal diffusivity of the wollastonite coating decreases slightly up to around 650 °C and then increases gradually. On the second thermal cycle, the thermal diffusivity of the coating increases by about 20% comparing with the first thermal cycle. The thermal diffusivity curves for the first and second thermal cycles are almost parallel.

4. Discussion

During atmospheric plasma spraying, wollastonite is rapidly heated, then rapidly cooled and solidified.[16] At high temperature, the wollastonite particles are partly or completely in molten state. The formation of SiO_2 in the coating possibly may be due to phase separation in CaO-SiO_2-based melt during solidification. At the same time, it is possible that CaO-SiO_2-based glassy phase with low silicon content is also formed in the coating resulting from phase separation. Kolman et al.[17] reported that β-Ca_2SiO_4 was found in the plasma sprayed wollastonite coating. However, β-Ca_2SiO_4 was not found in Fig. 3, which may be because Ca_2SiO_4 exists in glassy phase form. In addition, with the very small particles of the wollastonite powder, overheating and vaporization may lead to decomposition to form compounds such as SiO_2 and CaO. According to the results of Fig. 2 and 3, Peer Reviewed

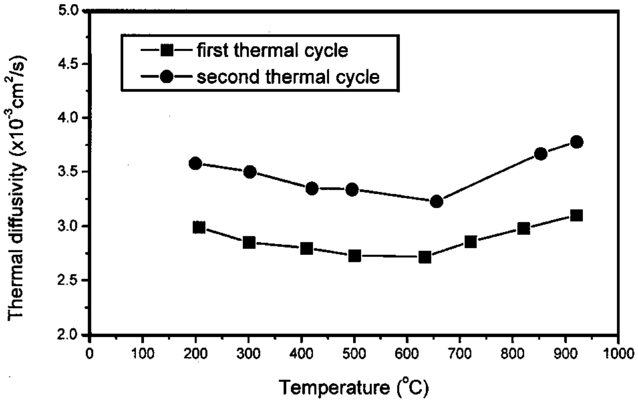

Fig. 5 The thermal diffusivity of the wollastonite coating during the first and second thermal cycles

it is clear that tridymite likely reacts with other composites such as CaO and glassy phase to form crystalline wollastonite when the coating is heated at about 882 °C.

High residual stresses developed in the as-sprayed thick coating during the plasma spraying process. The residual stress in the thick wollastonite coating will relax by plastic deformation when the coating is heated over 700 °C. Therefore, the decrease in the CTE between 700 °C and approximately 850 °C during the first cycle is mainly attributed to the stress relaxation. With the temperature increasing up to 850 °C, the stress relaxes completely. Therefore, the coating will stop contracting and expand gradually with the increase in temperature. During the second thermal cycle, the CTE of the coating increases slightly with the increase in temperature from room temperature to 1000 °C, resulting from a lack of residual stress in the coating.

After the heat treatment at 900 °C for 1 h, the wollastonite coating on Ti-6Al-4V substrate did not separate from the substrate. This may be because the CTE of Ti-6Al-4V alloy (8.8×10^{-6}/°C) is close to that of the wollastonite coating (Fig. 4). During the heat treatment process, the expansion or contraction of the coating was nearly coincidental with that of the Ti-6Al-4V substrate, which means that the bonding between the coating and the substrate was still very good after the heat treatment.

Heat transfer in ceramics at low temperature comes from phonon conduction together with gas convection in pores.[18] Phonon scattering, which reduces thermal diffusivity, is mainly caused by phonon-phonon interactions, in pores, at grain boundaries and in contacts between lamellae. Gas convection in pores increases with the increase in temperature of the coating, whereas phonon conduction decreases with the increase in temperature of the coating, owing to the increase in phonon scattering. Therefore, the thermal diffusivity of the coating decreases slightly with the increase in the temperature of the coating at low temperature. The increase in the thermal diffusivity of the coating in high temperature is attributed to the gases in the pores, such as in microcracks and the nonbonded interface area. This is because the heat transfer from convection of gases and radiation between lamellae will increase the apparent effective thermal diffusivity.[19] Microstructure and phase changes take place in the coating after the first thermal cycle, which means that the thermal diffusivity increases by about 20% on the second thermal cycle compared with that of the first thermal cycle.

5. Conclusions

Atmospheric plasma sprayed wollastonite coating was characterized by slight lamellar structure with a few pores and microcracks. Crystalline wollastonite, glassy phase, and tridymite (SiO_2) were observed in the coating. Tridymite (SiO_2) likely reacted with other compounds such as CaO and glassy phase to form crystalline wollastonite when the coating was heated at about 882 °C.

The thermophysical properties of the coating were obviously different between the first and second thermal cycles. During the first thermal cycle, there was an obvious contraction from 700-850 °C because of the stress relaxation. The thermal diffusivity of the wollastonite coating was $2.7\text{-}3.1 \times 10^{-3}$cm^2/s. During the second thermal cycle, the CTE of the wollastonite coating increased slightly between room temperature and 1000 °C. The thermal diffusivity of the coating increased by about 20% compared with that of the first thermal cycle. The bonding between the coating and Ti-6Al-4V substrate was always very good before and after the heat treatment. Therefore, atmospheric plasma sprayed wollastonite coating may be used as thermal barrier coating on substrates such as titanium and titanium alloys.

Acknowledgments

This work is supported by National Basic Research Fund under grant G1999064701 and Shanghai Science and Technology R&D Fund under grant 995211020.

References

1. W.A. Deer, R.A. Howie, and J. Zussman: In *Chain Silicates*, Longmans, Green, London, 1963, pp. 167-75.
2. M. Vukovich: "Effect of Wollastonite Substitute in a Semivitreous Dinnerware Body," *J. Am. Ceram. Soc.*, 1956, *39*, pp. 323-29.
3. K.C. Rieger: "Wollastonite," *Am. Ceram. Soc. Bull.*, 1995, *74*, pp. 160-61.
4. V.H. Remington, "Wollastonite as a Ceramic Materials," *Am. Ceram. Soc. Bull.*, 33, 1954, p. 312.
5. S. Hayashi, N. Otsuka, K. Akiyama, K. Okada, and T. Yano: "Preparation of Diopside Fine Powders by Spray Pyrolysis and Its Sinterability," *J. Ceram. Soc. Jpn.*, 1989, *97*, pp. 742-46.
6. P.N. De Aza, F. Guitian, and S. De Aza: "Bioactivity of Wollastonite Ceramics: In Vitro Evaluation," *Scr. Metall. Mater.*, 1994, *31*, pp. 1001-05.
7. P.N. De Aza, F. Guitian, and S. De Aza: "Morphological Studies of Pseudo-Wollastonite for Biomedical Application," *J. Microsc.*, 1996, *182*, pp. 24-31.
8. P.N. De Aza, F. Guitian, and S. De Aza: "Bioeutectic: A New Ceramic Material for Human Bone Replacement," *Biomaterials*, 1997, *18*, pp. 1285-91.
9. P.N. De Aza, F. Guitian, and S. De Aza: "Reactivity of Wollastonite-Tricalcium Phosphate Bioeutectic Ceramic in Human Parotid Saliva," *Biomaterials*, 2000, *21*, pp. 1735-41.
10. M. Begghini, L. Bertini, and F. Frendo: "Thermal Expansion of Thermally Sprayed Coatings" in *Proceedings of the 15th International Thermal Spray Conference*, Nice, France, C. Coddet, ed., ASM International, 1998, pp. 1595-99.
11. Y.-K. Lee, H.-J. Kim, and R.-W. Chang: "Thermal Expansion Properties of Plasma-Sprayed Thick Coatings" in *Proceedings of the 15th International Thermal Spray Conference*, Nice, France, C. Coddet, ed., ASM International, 1998, pp. 1629-34.
12. R.E. Taylor, X. Wang, and X. Xu: "Thermophysical Properties of Thermal Barrier Coatings," *Surf. Coat. Technol.*, 1999, *120-121*, pp. 89-95.
13. T.A. Taylor: "Thermal Properties and Microstructure of Two Thermal Barrier Coatings," *Surf. Coat. Technol.*, 1992, *54-55*, pp. 53-57.
14. F. Cernuschi, P. Binachi, M. Leoni, and P. Scardi: "Thermal Diffusivity/

Microstructure Relationship in Y-PSZ Thermal Barrier Coatings," *J. Therm. Spray Technol.*, 1999, *8*, pp. 102-09.

15. "ASTM C633-Standard Method of Test for Adhesive or Cohesive Strength of Flame-Sprayed Coatings" in *19th Annual Book of ASTM Standards*, Part 17, American Society for Testing and Materials, Philadelphia, PA, 1969, pp. 636-42.
16. R. McPherson: "The Relationship Between the Mechanism of Formation, Microstructure and Properties of Plasma-Sprayed Coatings," *Thin Solid Films*, 1981, *83*, pp. 297-310.
17. B.J. Kolman, K. Neufuss, J. Havský, J. Ddubský, and P. Chráskka: "Chemical Inhomogenicity of Silicates Treated by Plasma Spraying," *J. Anal. At. Spectrom.*, 1999, *14*, pp. 471-73.
18. W.D. Kingery, H.K. Bowen, and D.R. Bowen: in *Introduction to Ceramics*, 1st ed., John Wiley & Sons, New York; 1960, p. 486.
19. A. Ohmori and C.-J. Li: "The Structure of Thermally Sprayed Ceramic Coatings and Its Dominant Effect on the Coating Properties" in *Plasma Spraying*, R. Suryanarayanan, ed., World Scientific, Singapore, 1993, pp. 179-200.